Food Chemistry: X 11 (2021) 100128

Contents lists available at ScienceDirect

Food Chemistry: X

journal homepage: www.sciencedirect.com/journal/food-chemistry-x

Application of spectral features for separating homochromatic foreign matter from mixed congee

Jiyong Shi *, Yueying Wang, Chuanpeng Liu, Zhihua Li, Xiaowei Huang, Zhiming Guo, Xinai Zhang, Di Zhang, Xiaobo Zou *

Agricultural Product Processing and Storage Lab, School of Food and Biological Engineering, Jiangsu University, Zhenjiang, Jiangsu 212013, China

ARTICLE INFO

Keyword:
Mixed congee
Homochromatic foreign matter
Hyperspectral imaging technology
Pattern recognition
Chemometrics

ABSTRACT

Foreign matter (FM) in mixed congee not only reduces the quality of the congee but may also harm consumers. However, the common computer vision methods with poor recognition ability for the homochromatic FM. This study used hyperspectral reflectance images with the pattern recognition model to detect homochromatic FM on the mixed congee surface. First, spectral features corresponding to homochromatic FM and background were extracted from hyperspectral images. Then, based on the optimal spectral preprocessing method, LDA, K-nearest neighbor, backpropagation artificial neural network, and support vector machine (SVM) were used to classify the spectral features. The results revealed that the SVM model input with raw spectra principal components exhibited optimal identification rates of 99.17%. Finally, most of the pixels for homochromatic FM were classified correctly by using the SVM model. To summarized, hyperspectral images combined with pattern recognition are an effective method for recognizing homochromatic FM in mixed congee.

1. Introduction

In modern society, people are becoming increasingly conscious regarding their diet and nutrition. Various coarse grains are typically mixed to prepare healthy food. Mixed congee is fast becoming a common ingredient in kitchens because of its high nutritional value and cooking convenience (Xiao-Feng, Cheng-Xiang, Jian, Fu-Jun, Shu-Hong, & Sheng-Lin, 2019). The best-selling mixed congee on shopping websites is displayed in Fig. S1. However, such as stones, hulls, leaves, and packaging plastics, inevitably mix with mixed congee during transportation and packaging. Foreign matter (FM) contamination is a vital quality index because the consumption of mixed congee contaminated with FM can cause physical harm and psychological distress to consumers. Consequently, FM contamination has become a prominent problem in food safety (Caporaso, Whitworth, & Fisk, 2018; Reinholds, Bartkevics, Silvis, van Ruth, & Esslinger, 2015).

The computer vision (CV) method is typically used to identify FM during the industrial production of beans and rice. In this method, foreign objects are identified using color and shape differences between safe food and FM-contaminated food (Oliveira, Cerqueira, Barbon, & Barbin, 2021; Pearson, 2010). Image segmentation is performed to isolate FM. Although CV can identify FM accurately and effectively, it cannot provide accurate optical features of homochromatic FM. If the color and shape of FM are the same as that of mixed porridge, this will result in FM being incorrectly classified as mixed porridge. Therefore, it is difficult to identify FM using CV when the color and shape of FM are semblable with food.

Previous studies have demonstrated that spectral features are sensitive to the chemical components of agricultural products (Sheibani et al., 2014). Moreover, spectral techniques based on visible (VIS) (Herrero-Latorre, Barciela-García, García-Martín, & Peña-Crecente, 2019; Monago-Maraña, Eskildsen, Galeano-Díaz, Muñoz de la Peña, & Wold, 2021; Shi et al., 2019), near-infrared (NIR) (Biancolillo, Firmani, Bucci, Magrì, & Marini, 2019; Firmani, De Luca, Bucci, Marini, & Biancolillo, 2019; Piarulli et al., 2020; Rodionova, Fernández Pierna, Baeten, & Pomerantsev, 2021), and mid-infrared (MIR) spectra (Aykas & Menevseoglu, 2021; Aykas & Rodriguez-Saona, 2016; Botelho, Reis, Oliveira, & Sena, 2015) have been successfully used for the qualitative analysis of the chemical composition of various agricultural products. The chemical composition of homochromatic FM and mixed congee differs considerably, and accordingly, the use of spectral features to discriminate FM with similar colors to those of mixed congee is reasonable.

Acquiring the spectral data of the entire mixed congee sample pixel

* Corresponding author.
E-mail addresses: shi_jiyong@ujs.edu.cn (J. Shi), zou_xiaobo@ujs.edu.cn (X. Zou).

https://doi.org/10.1016/j.fochx.2021.100128
Received 9 April 2021; Received in revised form 15 August 2021; Accepted 19 August 2021
Available online 21 August 2021

by pixel is critical for the proposed method. Unlike conventional spectral technologies, such as VIS, NIR, and MIR, which rely on spot measurement, hyperspectral imaging (HSI) technology combines conventional spectroscopy and imaging techniques to acquire the spectra for each pixel in the two-dimensional image of an object (Shan et al., 2018; Zhang, Li, Zhang, & Rodgers, 2016). In addition to the analysis of the chemical composition of the sample, accurate spectral and spatial data should be acquired from the sample surface (Zhang, Li, & Yang, 2017). HSI technology satisfies these requirements and has been successfully used to detect FM such as plastics, branches, and leaves in agricultural products (Serranti, Palmieri, Bonifazi, & Cózar, 2018; Torres, Sánchez, Cho, Garrido-Varo, & Pérez-Marín, 2019; Zhang, Li, Zhang, & Rodgers, 2016; Zhu et al., 2020;). Therefore, the spectral data of the entire mixed congee sample can be acquired pixel by pixel by using HSI technology to realize the recognition of homochromatic FM.

A high-precision method was proposed in this study for automatically distinguishing homochromatic FM from mixed congee. The spectral features of mixed congee contaminated with homochromatic FM were acquired from the hyperspectral image to identify homochromatic FM from mixed congee automatically (Manfredi et al., 2018). The performance of various pattern recognition models was compared using the proposed method (Rodionova et al., 2021). Finally, the output of the optimal pattern recognition model at each pixel was combined with digital image processing technology to discriminate the homochromatic FM from the mixed congee background. The purpose of this study was to enable the computer vision method to accurately distinguish FM that are similar in color to mixed congee. Through accurate homochromatic FM detection, the quality and safety in the mixed congee production process can be effectively controlled.

2. Materials and methods

2.1. Sample preparation

Typically, mixed congee comprises glutinous rice, mung bean, red bean, millet, black rice, and barley. In this study, six types of FM, namely red plastic (color similar to that of red bean), green leaf (color similar to that of mung bean), stone (color similar to that of barley), white plastic (color similar to that of glutinous rice), black rubber (color similar to that of black rice), and hull (color similar to that of millet), were considered for research [Fig. 1(a)]. Plastic FM comprises common packaging materials. Green leaves are typically picked when mung beans are harvested. The type of stone is concrete. Hulls are collected from the field. Black rubber typically originates from conveyor rings. The aforementioned FM was selected for this study because such FM commonly mixes with and contaminates mixed congee during its transportation, processing, and packaging. Furthermore, the color of such FM is similar to that of the raw materials used for preparing mixed congee. The mixed congee sample contaminated with homochromatic FM is displayed in Fig. 1(b). Two types of samples were prepared for the experiments. The first is the independent ingredients sample containing the corresponding FM. Each of the six mixed congee ingredients was prepared separately with 50 g without mixing, and corresponding types of FM were added in a 50:1 ratio. Each ingredients group was simultaneously set in five parallel, and thirty samples were prepared for the study. The other is the mixed congee sample containing all the FM. Six mixed congee ingredients were prepared with 50 g each and fully mixed, and all types of FM were added according to the ratio of 50:1.

2.2. Hyperspectral image acquisition

A line-scanning HSI system with a VIS/NIR wavelength range of 432–963 nm was used to acquire hyperspectral images of the prepared mixed congee samples in the reflectance mode. The hyperspectral imaging system consisted of a line-scanning spectrograph (ImSpector, VI0E, Spectra Imaging Ltd., Finland), a complementary metal-oxide semiconductor camera (BCi4-U-M−20−LP, Vector International, Belgium), two 150-watt illuminators (Fiber-Lite PL900-A, Dolan-Jenner Industries Inc., USA), a conveyor (Zolix TS200AB, Zolix. Corp., China), an enclosure (ZJgrt, Great Ltd., China), data acquisition and preprocessing software (Spectra Cube, Auto Vision Inc., USA), and a computer (HPdx2390MT, Hewlett-Packard, China), as displayed in Fig. S2 (a). The exposure time of the camera was 50 ms, and the speed of the conveyor was 0.9 mm/s. Detailed information regarding hyperspectral image collection is presented in our earlier study (Shi et al., 2017, 2018).

2.3. Spectral data processing

After hyperspectral imaging, the images of the mixed congee sample were digitized into pixels containing spectral data, and the homochromatic FM was segmented from the mixed congee background based on the spectral features of the pixels. The HSI system was used to acquire the three-dimensional (3D) data cube of the mixed congee samples [Fig. S2(b)]. The *x*-axis and *y*-axis indicate the pixel location, and the λ-axis indicates the wavelength of each image. Thus, the 3D data cube contained spectral data and image data of the mixed congee samples. The individual pixel data were extracted from the 3D data cube. Next, all the signal values of the pixel were presented in a curve in the order of their wavelengths. The surface of the mixed congee sample was digitized accurately by using the pixels in Fig. S2(b), and the sample properties at

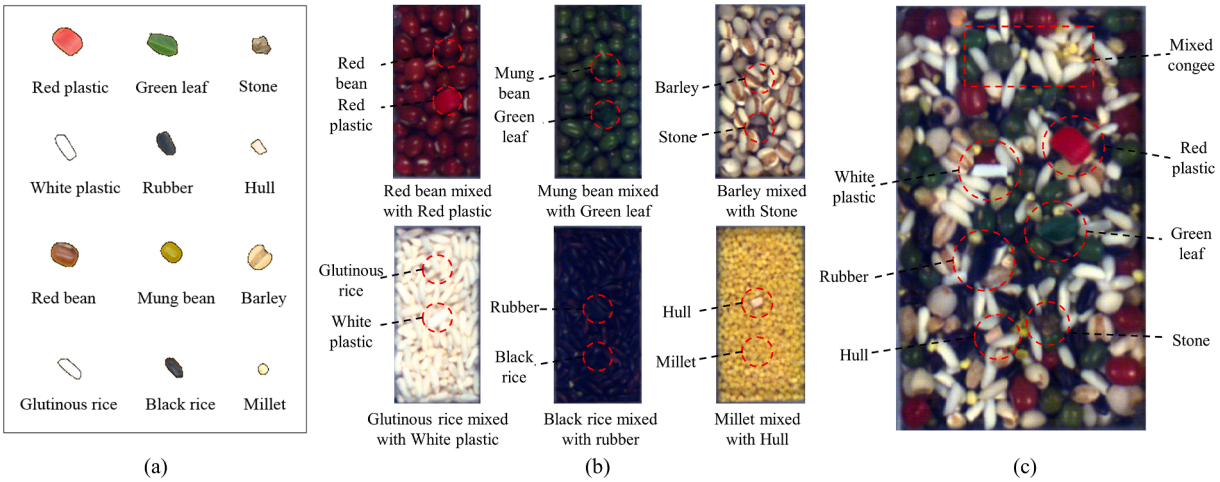

Fig. 1. (a) Mixed congee comprising six raw materials with six types of FM; (b) six types of mixed congee raw materials mixed with homochromatic FM; and (c) mixed congee mixed with six types of FM.

each pixel were rapidly determined using its spectral information, which enabled the identification of FM areas and mixed congee background areas by using spectral features.

The acquired hyperspectral images were corrected by applying Equation (1). White reference images were acquired from the white spectral data for a panel with 99% reflectance, and dark images were acquired by covering the lens of the camera completely.

$$R\lambda = \frac{I\lambda - B\lambda}{W\lambda - B\lambda} \quad (1)$$

where I_λ is the intensity of the raw image, B_λ is the intensity of the dark image, W_λ is the intensity of the white reference image, and R_λ is the intensity of the corrected image.

Chemometric methods were used to facilitate the establishment of pattern recognition models (Biancolillo & Marini, 2018; Rodionova, Fernández Pierna, Baeten, & Pomerantsev, 2021; Zhang, Liu, He, & Li, 2012; Ballabio and Davide, 2009). In addition to containing beneficial information, raw spectral data contain useless information and noise interference information, such as the baseline drift and high-frequency noise, due to the effect of nonsample information, such as environmental information and machine operating conditions. Therefore, the preprocessing of raw spectral data is critical for removing useless information and improving the accuracy and stability of modeling (Shi et al., 2019). In this study, the best spectral preprocessing method was selected from among standard normal variable transformation, the Savitzky–Golay (SG) method, vector normalization, the first-derivative method, the second-derivative method, and multiple scatter correction.

Hyperspectral datasets provide considerable data and rich band information. However, not every band is sensitive to FM. The correlation between the bands is too large and contains redundant information (Shi et al., 2012). Therefore, compressing the spectral data to eliminate insensitive and redundant bands for reducing the data dimension as well as reducing the complexity of operations and classification models are critical tasks. Principal component analysis (PCA) was used to eliminate the multicollinearity in the original data, and an orthogonal transformation was used to replace the original variables (wavelengths) with fewer principal components (PCs) to maximize the representation of the original data (Jolliffe, 2002). The (SPA) is an emerging band extraction method. Each selected band has the smallest linear relationship with the previously selected band (Milanez, Araújo Nóbrega, Silva Nascimento, GalvãO, & Pontes, 2017). A band combination was selected to maximize the representation of the original data by minimizing the root mean square error (RMSE).

The samples were divided into a calibration dataset and prediction dataset in a 2:1 ratio. The SPA and PCA were used to extract the spectral features of the FM and background pixels from the calibration dataset. The linear discriminant analysis (LDA) (Furlanetto et al., 2020), K-nearest neighbor (KNN) (Yahui, Xiaobo, Tingting, Jiyong, & Holmes, 2017), backpropagation artificial neural network (BP-ANN) (Niu, Shao, Zhao, & Zhang, 2012), and support vector machine (SVM) algorithms (Bazi & Melgani, 2006; Chen, Zhao, Fang, & Wang, 2007) were used to construct pattern recognition models for identifying homochromatic FM in mixed congee. The raw spectra, SPA wavelength selection, and PCs of raw spectra were used as the model input variables. The calibration models were optimized using the spectral features of the prediction set. The optimal calibration model was validated using an independent testing dataset. The discrimination performance was evaluated according to the percentage of samples that were correctly classified (Xiaobo et al., 2011).

2.4. FM visualization

The steps for recognizing homochromatic FM in mixed congee are illustrated in Fig. 2. First, homochromatic FM and background spectra were measured. A region of interest (ROI) was defined within the FM and background areas, and the mean spectral data of the FM and background areas were then extracted for further data analysis. Second, pattern recognition models for homochromatic FM segmentation were constructed. PCA and the SPA were used to extract the spectral features of the FM and background pixels from the calibration dataset. Moreover, the LDA, KNN, BP-ANN, and SVM algorithms were used to construct segment models by correlating the spectral features with the origins (homochromatic FM or background areas) of the pixels. Image classification was conducted according to the following procedure. The optimal method was used to classify FM and mixed congee in the hyperspectral images. To evaluate the accuracy of the classification, truth ROIs from each type of FM were manually drawn on the image. The model output variable of the homochromatic FM area was set as 1, and the background area was set as 0. The output result was replaced with a binary image.

2.5. Software

Hyperspectral images of the mixed congee samples were collected using SpectralCube software (ImSpector, image, Auto Vision Inc., USA). All the hyperspectral image processing methods were performed in MATLAB 2016 (MathWorks, Natick, MA, USA).

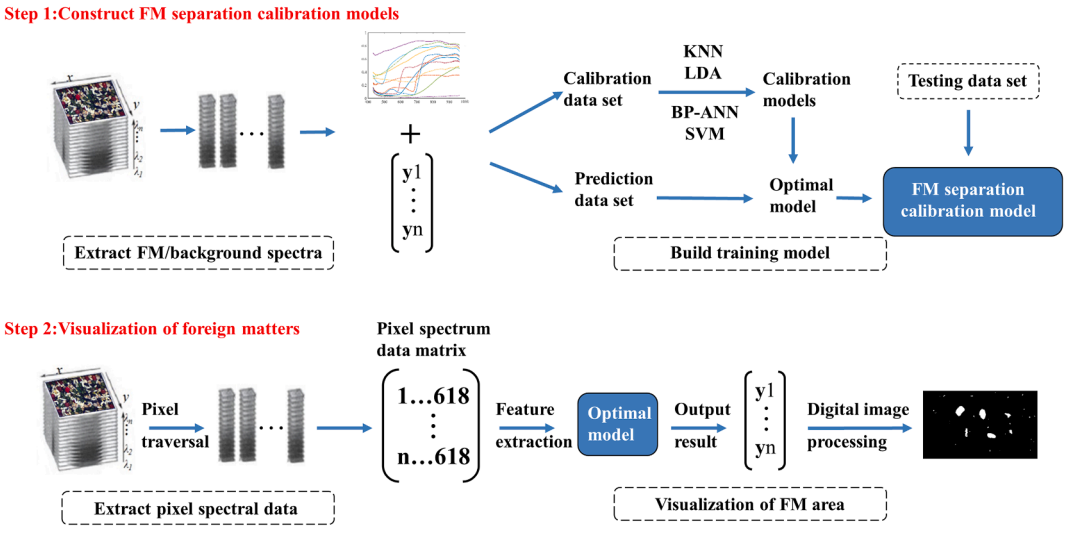

Fig. 2. Process flowchart for recognizing homochromatic FM in mixed congee.

3. Results and discussion

3.1. Spectral analysis

The ROIs for each type of FM and mixed congee were outlined using the ellipse and rectangular tool in ENVI and marked on the RGB image, as displayed in Fig. 3(a). The ROIs were then mapped onto the original hyperspectral images to extract the full spectra (432–963 nm), which were averaged to represent the mean spectrum of each ROI [Fig. 3(b)]. A total of 360 mean spectra from 30 samples (with 6 FM ROIs and 6 congee ROIs in each sample) were acquired. The normalized mean spectra (ranging from 0 to 1) indicated that considerable differences existed in the reflectance features of various types of FM and mixed congee ingredients [Fig. 3(b)]. Each mean spectrum of the FM and mixed congee samples was acquired by averaging the spectra of 30 samples within each category. The FM and mixed congee spectral curves revealed that the green leaf and mung beans exhibited a strong absorption peak at 680–690 nm. The absorption intensity of the stone spectrum was uniform in each band. White plastic exhibited a weak absorption peak at 690 nm. Black rubber strongly absorbed light and exhibited low reflectivity at all wavelengths. The spectral trend of the hull was similar to that of barley. Millet exhibited a strong absorption peak at 490 nm. Overall, the spectra of FM and mixed congee differed considerably. The spectral variation between FM and mixed congee indicated that spectral features can be used to distinguish FM from mixed congee.

3.2. Spectral feature extraction

According to the PCA results for the six types of FM and mixed congee ingredients in the full spectrum, the contribution rates of the first, second, and third principal components were 84.07%, 11.7%, and 2.84%, respectively. The cumulative contribution rate of the three principal component variables was 98.61%. In Fig. S3, blue represents mixed congee ingredients and red represents FM, 12 classes could be generally separated using the first three PCs. The PC score map was consistent with the spectral features of FM. Fig. S4 displays the RMSEs and feature wavelengths obtained through SPA. Feature wavelength extraction was performed for accurately classifying FM and mixed congee with few feature wavelengths. As displayed in Fig. S4(a), when the number of feature wavelengths was 7, the RMSE was 0.045, which did not significantly different from the RMSE when the number of feature wavelengths was 3. Therefore, the first three feature wavelengths were selected as the optimal results according to their contribution to the classification result [Fig. S4(b)]. The corresponding wavelengths of the 222nd, 167th, and 284th feature wavebands in this dataset were 617.29, 570.32, and 670.64 nm, respectively.

3.3. Build calibration models

A total of 180 spectra each of FM and mixed congee were extracted from the hyperspectral images. The spectra of the FM were categorized in the foreground category, whereas the spectra of mixed congee were categorized in the background category. Foreground samples were defined as “positives (P)” and background samples were defined as “negatives (N)”. The spectral data of the foreground and background samples and their categories were used to construct an FM area segment model, as described in Section 2.4. Table 1 presents the prediction results of the LDA models constructed using each preprocessing spectrum. The recognition rates of these models vary greatly. The LDA model constructed using the SG smoothing exhibited the highest recognition accuracy. The correct identification rates (Ir) of the calibration and prediction sets were 93.88% and 94.17%, respectively, for the aforementioned model. Therefore, the SG smoothing was selected as the preprocessing method in the subsequent data processing.

The LDA, KNN, BP-ANN, and SVM algorithms were used to construct segmentation models of the FM area. The full-band spectrum, feature-band spectrum, and PC variables after SG preprocessing were the input variables of the pattern recognition models. The BP-ANN model was set as follows: the number of output layer units was as 2 (FM and mixed congee), the hyperbolic tangent function was set as the transfer function of the model, the initial weight was set as 0.9, the momentum factor and learning factor were set as 0.1, the convergence error was set as 0.0002, and the number of training iterations was set as 2000. In the

Table 1
Accuracy of the linear discriminant analysis models under various preprocessing methods (%).

Methods	PCs	Calibration set	Validation set
MSC[a]	3	57.08	59.17
2ND [b]	4	57.08	62.50
1ST [c]	3	63.75	65.83
VN [d]	3	73.75	73.33
SNVT [e]	6	90.42	91.67
SG [f]	8	93.88	94.17

[a] Multiplicative scatter correction;
[b] 2nd derivative;
[c] 1st derivative;
[d] Vector normalization;
[e] Standard normalized variate transform;
[f] Savitzky-Golay.

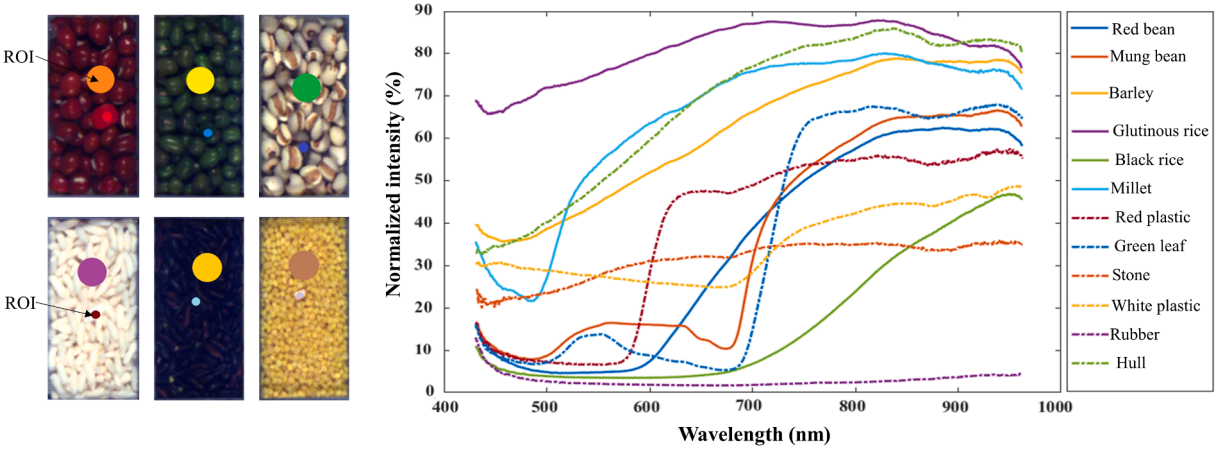

Fig. 3. (a) Regions of interest (ROIs) defined on the hyperspectral image; (b) Normalized mean spectra of the ROIs.

SVM model, the regularization parameter of the optimal radial-basis kernel function was determined to be 2.33 by using the cross-validation method.

The capability of the optimal calibration modes for the segmentation of unknown samples was tested using an independent testing set. In total, 60 spectra each of FM and mixed congee was extracted from the hyperspectral images and used to construct the testing dataset. The results of the calibration models are summarized in Table 2. The recognition rate of PCA variable model was higher than that of SPA wavelength selection model, which indicated that the PCA variables represented more raw spectral information than SPA wavelength selection. The lowest recognition rate was achieved through raw spectra modeling, which revealed that the raw spectra contained considerable redundant information. Furthermore, the SVM model exhibited the best classification results. Under SVM modeling based on the PCA variables, the accuracy of the calibration set, prediction set, and test set were 98.33%, 99.17%, and 97.50% respectively, which could be attributed to the higher nonlinear intensity changes in the fused data than in the linear data. The SVM model is superior to other models in processing nonlinear data. Thus, the SVM model based on PCA variables achieved a high capability for the separation of an unknown sample. The recognition results based on PCA variables also indicated that the spectral features corresponding to the foreground or background samples were successfully characterized using the optimized identification model.

Table 2
Results of the calibration models for FM separation.

Spectra treatment	Raw spectra	SPA wavelength selection	PCA variables		
LDA	Calibration set	Ir(%)	90.28	91.67	93.88
	Validation set	Ir(%)	89.17	90.00	94.17
	Testing set	Ir(%)	88.34	93.33	92.50
		TP [a]	54	56	57
		FN [b]	6	4	3
		TN [c]	52	56	54
		FP [d]	8	4	6
KNN	Calibration set	Ir(%)	88.83	89.44	92.50
	Validation set	Ir(%)	86.39	88.33	91.67
	Testing set	Ir(%)	85.83	90.00	90.83
		TP	52	55	57
		FN	8	5	3
		TN	51	53	52
		FP	9	7	8
BP-ANN	Calibration set	Ir(%)	93.33	94.72	97.50
	Validation set	Ir(%)	88.89	90.00	90.83
	Testing set	Ir(%)	92.50	94.17	95.00
		TP	57	58	59
		FN	3	2	1
		TN	54	55	55
		FP	6	5	5
SVM	Calibration set	Ir(%)	94.44	95.83	98.33
	Validation set	Ir(%)	95.00	96.11	99.17
	Testing result	Ir(%)	92.50	97.50	97.50
		TP	57	59	59
		FN	3	1	1
		TN	54	58	58
		FP	6	2	2

[a] True positive;
[b] false negative;
[c] True negative;
[d] False positive.

3.4. Image classification

A 150 × 150-pixel hyperspectral image was selected [Fig. 4(a)]. The truth ROIs for each FM category were selected and marked with various colors, as displayed in Fig. 4(b). On the initial classification map [Fig. 4 (c)], the majority of the pixels within each class were correctly classified. After conducting morphological image processing by using an average filter (kernel = 3 × 3 pixels), most of the noise was removed [Fig. 4(d)]. Most misclassifications occurred between green leaf and mung bean. Many pixels of mung bean were misclassified as green leaf, which could be attributed to the similar chemical composition of green leaves and mung beans.

To verify the accuracy of the FM-separation model, six types of FM were randomly placed on the surface of mixed congee for recognition (Fig. S5). The computer vision method and hyperspectral method were used to separate FM. The HSV color mode matches people's perceptions of colors. "H" stands for chromaticity, "S" stands for saturation, and "V" stands for brightness. Fig. S5(b) depicts the separated images for each channel. As displayed in Fig. S5(c), from the perspective of chromaticity, distinguishing FM from colorful mixed congee was difficult. From the perspective of saturation, with the exception of red plastic, whose chromaticity value is marginally higher than that of red beans, distinguishing other types of FM from the mixed congee ingredients with the same color as the FM was difficult. From the perspective of brightness, separating high-brightness glutinous rice and white plastic from mixed congee was effortless; however, separating white plastic from glutinous rice was difficult due to the similarity in their brightness. These results revealed that establishing a threshold to distinguish FM from mixed congee is difficult, and all 30 samples were misjudged. The detection rate for the six types of FM was 0%. Fig. S5(e) reveals that after FM separation by using hyperspectral features, only FM appeared in the foreground region and mixed congee was successfully identified as the background. However, many misjudged noise points occurred. The results obtained after the morphological expansion and corrosion noise reduction operations are also illustrated in Fig. S5(e). These results indicated that hyperspectral features could differentiate FM from mixed congee even when the colors of mixed congee were similar to those of FM.

4. Conclusion

A novel method is proposed in this study to separate homochromatic FM from mixed congee using hyperspectral imaging technology. Various congee and FM with colors and shapes similar to those of congee were employed to collect hyperspectral image data. The spectral features of congee and FM were extracted from the hyperspectral images and employed to construct calibration models for separating FM from congee and mixed congee. With the aid of calibration models, each pixel of a mixed congee hyperspectral image was identified according to its spectral features. An accuracy of more than 97% was achieved in classifying six types each of FM and mixed congee by using an SVM classification model based on PCA variables. Compared with the conventional computer vision method, the proposed method more effectively identified homochromatic FM to that of congee and is therefore of practical importance.

CRediT authorship contribution statement

Jiyong Shi: Methodology, Writing - original draft, Funding acquisition. **Yueying Wang:** Conceptualization, Methodology, Writing - review & editing. **Chuanpeng Liu:** Investigation, Data curation. **Zhihua Li:** Validation, Investigation. **Xiaowei Huang:** Formal analysis. **Zhiming Guo:** Software. **Xinai Zhang:** Resources. **Di Zhang:** Validation. **Xiaobo Zou:** Supervision.

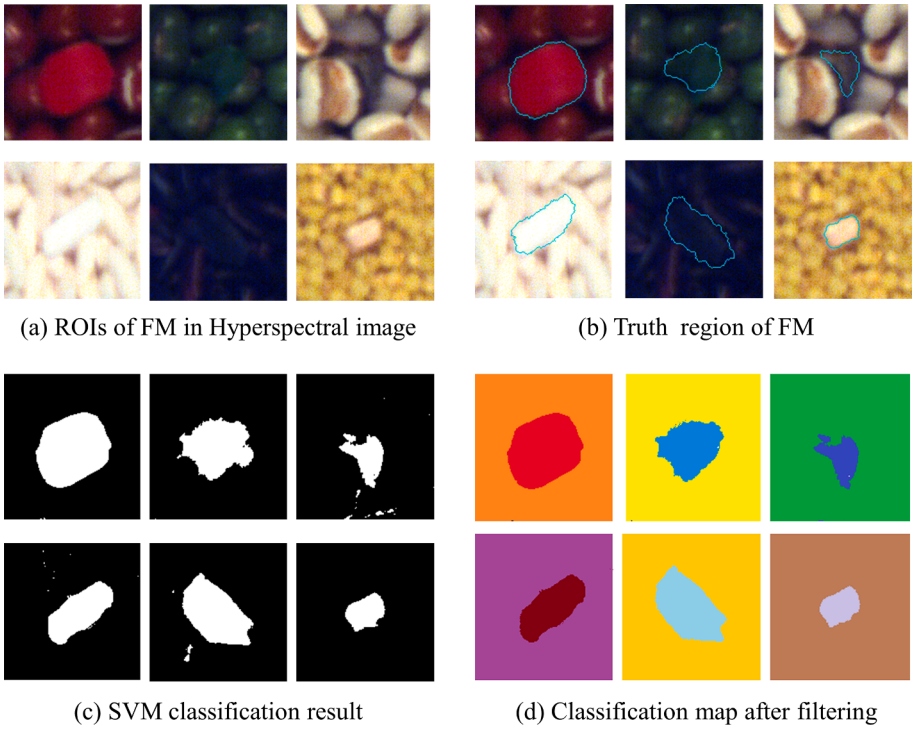

Fig. 4. Pixel-level image classification of FM by using the support vector machine algorithm.

Declaration of Competing Interest

The authors declare that they have no known competing financial interests or personal relationships that could have appeared to influence the work reported in this paper.

Acknowledgements

The authors gratefully acknowledge the financial support provided by the National Key Research and Development Program of China (grant number 2017YFC1600805), the National Natural Science Foundation of China (grant numbers 31772073, 31671844); the Natural Science Foundation of Jiangsu Province (grant number BE2019359).

Appendix A. Supplementary data

Supplementary data to this article can be found online at https://doi.org/10.1016/j.fochx.2021.100128.

References

Sheibani, A., Bahraman, N., & Sadeghi, F. (2014). FT-IR Application for the Detection of Pistachio Oil Adulteration. *Oriental Journal of Chemistry, 30*(3), 1205–1209.

Aykas, D. P., & Rodriguez-Saona, L. E. (2016). Assessing potato chip oil quality using a portable infrared spectrometer combined with pattern recognition analysis. *Analytical Methods, 8*(4), 731–741.

Aykas, D. P., & Menevseoglu, A. (2021). A rapid method to detect green pea and peanut adulteration in pistachio by using portable FT-MIR and FT-NIR spectroscopy combined with chemometrics. *Food Control, 121*, 107670. https://doi.org/10.1016/j.foodcont.2020.107670.

Ballabio, & Davide. (2009). Chapter 4 - Multivariate Classification for Qualitative Analysis. Infrared Spectroscopy for Food Quality Analysis and Control, 83-104. San Diego: Academic Press.

Bazi, Y., & Melgani, F. (2006). Toward an Optimal SVM Classification System for Hyperspectral Remote Sensing Images. *IEEE Transactions on Geoence & Remote Sensing, 44*(11), 3374–3385.

Biancolillo, Alessandra, Firmani, Patrizia, Bucci, Remo, Magrì, Andrea, & Marini, Federico (2019). Determination of insect infestation on stored rice by near infrared (NIR) spectroscopy. *Microchemical Journal, 145*, 252–258.

Biancolillo, A., & Marini, F. (2018). Chapter Four - Chemometrics Applied to Plant Spectral Analysis. *Comprehensive Analytical Chemistry, 80*, 69–104.

Botelho, Bruno G., Reis, Nádia, Oliveira, Leandro S., & Sena, Marcelo M. (2015). Development and analytical validation of a screening method for simultaneous detection of five adulterants in raw milk using mid-infrared spectroscopy and PLS-DA. *Food Chemistry, 181*, 31–37.

Caporaso, Nicola, Whitworth, Martin B., & Fisk, Ian D. (2018). Near-Infrared spectroscopy and hyperspectral imaging for non-destructive quality assessment of cereal grains. *Applied Spectroscopy Reviews, 53*(8), 667–687.

Chen, Quansheng, Zhao, Jiewen, Fang, C. H., & Wang, Dongmei (2007). Feasibility study on identification of green, black and Oolong teas using near-infrared reflectance spectroscopy based on support vector machine (SVM). *Spectrochimica Acta Part A Molecular and Biomolecular Spectroscopy, 66*(3), 568–574.

Firmani, Patrizia, De Luca, Silvia, Bucci, Remo, Marini, Federico, & Biancolillo, Alessandra (2019). Near Infrared (NIR) spectroscopy-based classification for the authentication of Darjeeling black tea. *Food Control, 100*, 292–299.

Furlanetto, Renato Herrig, Moriwaki, Thaise, Falcioni, Renan, Pattaro, Mariana, Vollmann, Alessandra, Sturion Junior, Antonio Carlos, … Nanni, Marcos Rafael (2020). Hyperspectral reflectance imaging to classify lettuce varieties by optimum selected wavelengths and linear discriminant analysis. *Remote Sensing Applications Society and Environment, 20*, 100400. https://doi.org/10.1016/j.rsase.2020.100400.

Herrero-Latorre, C., Barciela-García, J., García-Martín, S., & Peña-Crecente, R. M. (2019). Detection and quantification of adulterations in aged wine using RGB digital images combined with multivariate chemometric techniques. *Food Chemistry: X, 3*, Article 100046.

Jolliffe, I. T. (2002). Principal Component Analysis. *Journal of Marketing Research, 87*(4), 513.

Manfredi, Marcello, Robotti, Elisa, Quasso, Fabio, Mazzucco, Eleonora, Calabrese, Giorgio, & Marengo, Emilio (2018). Fast classification of hazelnut cultivars through portable infrared spectroscopy and chemometrics. *Spectrochim Acta A Mol Biomol Spectrosc, 189*, 427–435.

Milanez, Karla Danielle Tavares Melo, Araújo Nóbrega, Thiago César, Silva Nascimento, Danielle, Galvão, Roberto Kawakami Harrop, & Pontes, Márcio José Coelho (2017). Selection of robust variables for transfer of classification models employing the successive projections algorithm. *Analytica Chimica Acta, 984*, 76–85.

Monago-Maraña, O., Eskildsen, C. E., Galeano-Díaz, T., Muñoz de la Peña, A., & Wold, J. P. (2021). Untargeted classification for paprika powder authentication using visible – Near infrared spectroscopy (VIS-NIRS). *Food Control, 121*, Article 107564.

Niu, X. Y., Shao, L. M., Zhao, Z. L., & Zhang, X. Y. (2012). Nondestructive Discrimination of Strawberry Varieties by NIR and BP-ANN. *Spectroscopy & Spectral Analysis, 32*(8), 2095–2099.

Oliveira, M. M., Cerqueira, B. V., Barbon, S., & Barbin, D. F. (2021). Classification of fermented cocoa beans using computer vision. *Journal of Food Composition and Analysis, 97*(9), Article 103771.

Pearson, T. (2010). High-Speed Sorting of Grains by Color and Surface Texture. *Applied Engineering in Agriculture, 26*(3), 499–505.

Piarulli, Stefania, Sciutto, Giorgia, Oliveri, Paolo, Malegori, Cristina, Prati, Silvia, Mazzeo, Rocco, & Airoldi, Laura (2020). Rapid and direct detection of small microplastics in aquatic samples by a new near infrared hyperspectral imaging (NIR-

HSI) method. *Chemosphere, 260*, 127655. https://doi.org/10.1016/j.chemosphere.2020.127655.

Reinholds, Ingars, Bartkevics, Vadims, Silvis, Isabelle C. J., van Ruth, Saskia M., & Esslinger, Susanne (2015). Analytical techniques combined with chemometrics for authentication and determination of contaminants in condiments: A review. *Journal of Food Composition and Analysis, 44*, 56–72.

Rodionova, O. Ye, Fernández Pierna, J. A., Baeten, V., & Pomerantsev, A. L. (2021). Chemometric non-targeted analysis for detection of soybean meal adulteration by near infrared spectroscopy. *Food Control, 119*, 107459. https://doi.org/10.1016/j.foodcont.2020.107459.

Serranti, Silvia, Palmieri, Roberta, Bonifazi, Giuseppe, & Cózar, Andrés (2018). Characterization of microplastic litter from oceans by an innovative approach based on hyperspectral imaging. *Waste Management, 76*, 117–125.

shan, Jiajia, Zhao, Junbo, Liu, Lifen, Zhang, Yituo, Wang, Xue, & Wu, Fengchang (2018). A novel way to rapidly monitor microplastics in soil by hyperspectral imaging technology and chemometrics. *Environmental Pollution, 238*, 121–129.

Shi, J.-Y., Zou, X.-B., Zhao, J.-W., Wang, K.-L., Chen, Z.-W., Huang, X.-W., … Holmes, M. (2012). Nondestructive diagnostics of nitrogen deficiency by cucumber leaf chlorophyll distribution map based on near infrared hyperspectral imaging. *Scientia Horticulturae, 138*(1), 190–197.

Shi, Jiyong, Li, Wenting, Zhai, Xiaodong, Guo, Zhiming, Holmes, Mel, Elrasheid Tahir, Haroon, & Zou, Xiaobo (2019). Nondestructive diagnostics of magnesium deficiency based on distribution features of chlorophyll concentrations map on cucumber leaf. *Journal of Plant Nutrition, 42*(20), 2773–2783.

Shi, Jiyong, Zhang, Fang, Wu, Shengbin, Guo, Zhiming, Huang, Xiaowei, Hu, Xuetao, … Zou, Xiaobo (2019). Noise-free microbial colony counting method based on hyperspectral features of agar plates. *Food Chemistry, 274*, 925–932.

Shi, Jiyong, Chen, Wu, Zou, Xiaobo, Xu, Yiwei, Huang, Xiaowei, Zhu, Yaodi, & Shen, Tingting (2018). Detection of triterpene acids distribution in loquat (Eriobotrya japonica) leaf using hyperspectral imaging. *Spectrochimica Acta Part a-Molecular and Biomolecular Spectroscopy, 188*, 436–442.

Shi, Jiyong, Hu, Xuetao, Zou, Xiaobo, Zhao, Jiewen, Zhang, Wen, Holmes, Mel, … Zhang, Xiaolei (2017). A rapid and nondestructive method to determine the distribution map of protein, carbohydrate and sialic acid on Edible bird's nest by hyper-spectral imaging and chemometrics. *Food Chemistry, 229*, 235–241.

Torres, Irina, Sánchez, María-Teresa, Cho, Byoung-Kwan, Garrido-Varo, Ana, & Pérez-Marín, Dolores (2019). Setting up a methodology to distinguish between green oranges and leaves using hyperspectral imaging. *Computers and Electronics in Agriculture, 167*, 105070. https://doi.org/10.1016/j.compag.2019.105070.

Xiao-Feng, H., Cheng-Xiang, W., Jian, W., Fu-Jun, M. A., Shu-Hong, M. A., & Sheng-Lin, D. (2019). *Nutrient Ingredients Analysis and in Vitro Activity Evaluation on A Mixed Germ Congee*. Food and Nutrition in China.

Xiaobo, Zou, Jiyong, Shi, Limin, Hao, Jiewen, Zhao, Hanpin, Mao, Zhenwei, Chen, … Holmes, Mel (2011). In vivo noninvasive detection of chlorophyll distribution in cucumber (Cucumis sativus) leaves by indices based on hyperspectral imaging. *Analytica Chimica Acta, 706*(1), 105–112.

Yahui, L., Xiaobo, Z., Tingting, S., Jiyong, S., & Holmes, M. (2017). Determination of Geographical Origin and Anthocyanin Content of Black Goji Berry (Lycium ruthenicum Murr.) Using Near-Infrared Spectroscopy and Chemometrics. *Food Analytical Methods, 10*(4), 1034–1044.

Zhang, Mengyun, Li, Changying, & Yang, Fuzeng (2017). Classification of foreign matter embedded inside cotton lint using short wave infrared (SWIR) hyperspectral transmittance imaging. *Computers and Electronics in Agriculture, 139*, 75–90.

Zhang, Ruoyu, Li, Changying, Zhang, Mengyun, & Rodgers, James (2016). Shortwave infrared hyperspectral reflectance imaging for cotton foreign matter classification. *Computers & Electronics in Agriculture, 127*, 260–270.

Zhang, X., Liu, F., He, Y., & Li, X. (2012). Application of Hyperspectral Imaging and Chemometric Calibrations for Variety Discrimination of Maize Seeds. *Sensors, 12*(12), 17234–17246.

Zhu, Chunmao, Kanaya, Yugo, Nakajima, Ryota, Tsuchiya, Masashi, Nomaki, Hidetaka, Kitahashi, Tomo, & Fujikura, Katsunori (2020). Characterization of microplastics on filter substrates based on hyperspectral imaging: Laboratory assessments. *Environmental Pollution, 263*, 114296. https://doi.org/10.1016/j.envpol.2020.114296.